Journal of Applied Mechanics and Technical Physics, Vol. 36, No. 2, 1995

CALCULATION OF THE CHARACTERISTICS OF CONJUGATE HEAT AND MASS TRANSFER DURING GAS INJECTION AND THERMOCHEMICAL ABLATION IN THE VEIL ZONE*

V. I. Zinchenko, A. G. Kataev, and A. S. Yakimov

UDC 536.46:536.245.022

It has been shown [1] that the injection of a gas from the surface of a spherical nose section not only promotes heat flow along the generatrix, but can also serve as an efficient technique for lowering the surface temperature in zones of maximum heat input. When the stagnation enthalpy and pressure after the injection zone increase, a thermochemical ablation regime can be attained in the region of the thermal veil. The characteristics of this regime are related to the flow parameters, the mass flow rate of the injected gas coolant, the thermophysical characteristics of the shell in the flow, and the geometry of the shell.

In this article we discuss the solution of the heating and thermochemical ablation problem in high-enthalpy, supersonic air flow past a spherically blunted cone, taking into account the various flow regimes in the boundary layer and gas injection from the surface of the nose section. We investigate the influence of the mass flow rate of the injected gas and lengthwise heat flow on the characteristics of conjugate heat and mass transfer and thermochemical ablation of a graphite conical section.

1. We seek the conjugate heat and mass transfer characteristics from the solution of the system of equations describing the variation of the average quantities in the boundary layer, the energy conservation equation for a porous spherical nose section, and the time-dependent heat conduction equation for the conical part of the shell in a moving frame associated with the thermochemical ablation front.

In Dorodnitsyn–Lees variables the system of boundary-layer equations taking into account the laminar, transition, and turbulent flow regions appears as follows in the natural coordinate frame attached to the outer surface of the shell:

$$\frac{\partial}{\partial\eta}\left(l\frac{\partial\bar{u}}{\partial\eta}\right)+f\frac{\partial\bar{u}}{\partial\eta}=\alpha\left(\bar{u}\frac{\partial\bar{u}}{\partial\xi}-\frac{\partial f}{\partial\xi}\frac{\partial\bar{u}}{\partial\eta}\right)+\beta\left(\bar{u}^2-\frac{\rho_e}{\rho}\right); \tag{1.1}$$

$$\frac{\partial}{\partial\eta}\left[\frac{l}{\mathrm{Pr}_\Sigma}\frac{\partial g}{\partial\eta}+\frac{u_e^2}{H_e}l\left(1-\frac{1}{\mathrm{Pr}_\Sigma}\right)\bar{u}\frac{\partial\bar{u}}{\partial\eta}\right]+f\frac{\partial g}{\partial\eta}=\alpha\left(\bar{u}\frac{\partial g}{\partial\xi}-\frac{\partial f}{\partial\xi}\frac{\partial g}{\partial\eta}\right); \tag{1.2}$$

$$p=\rho h\frac{\gamma_e-1}{\gamma_e}. \tag{1.3}$$

For a porous spherical shell ($0\le s\le s_1$), assuming that the filtering of the injected gas in the direction normal to the surface is a one-dimensional process, the heat-conduction equation in the given frame has the form

$$\rho_1 c_1(1-\varphi)\frac{\partial T}{\partial t}=\frac{1}{H_1 r}\left[\frac{\partial}{\partial s}\left(\frac{r}{H_1}\lambda_1(1-\varphi)\frac{\partial T}{\partial s}\right)+\frac{\partial}{\partial n_1}\left(rH_1\lambda_1(1-\varphi)\frac{\partial T}{\partial n_1}\right)\right]+(\rho v)_{1w}\frac{r_w}{rH_1}c_{pg}\frac{\partial T}{\partial n_1}. \tag{1.4}$$

For the conical part of the body ($s_1\le s\le s_\kappa$) the heat-conduction equation is

*This work has received financial support from the Russian Fundamental Research Foundation (Project Code 93-013-17286).

Scientific-Research Institute of Applied Mathematics and Mechanics, 634055 Tomsk. Translated from Prikladnaya Mekhanika i Tekhnicheskaya Fizika, No. 2, pp. 126-135, March–April, 1995. Original article submitted January 19, 1994; revision submitted April 5, 1994.

 0021-8944/95/3602-0258$12.50

$$\rho_2 c_2\left(\frac{\partial T}{\partial t}-\omega\frac{\partial T}{\partial n_1}\right)=\frac{1}{r}\left[\frac{\partial}{\partial s}\left(r\lambda_2\frac{\partial T}{\partial s}\right)+\frac{\partial}{\partial n_1}\left(r\lambda_2\frac{\partial T}{\partial n_1}\right)\right],\quad \omega=\frac{(\rho v)_{2w}}{\rho_2}. \tag{1.5}$$

We write the boundary and initial equations as follows:

$$\bar{u}(\xi,\infty)=g(\xi,\infty)=1; \tag{1.6}$$

$$\bar{u}(\xi,0)=0,\qquad f(0,\xi)=f_w=-\frac{\int_0^\xi(\rho v)_w r_w\,d\xi}{\left(\frac{2}{R_N}\int_0^\xi\rho_e\mu_e u_e r_w^2\,d\xi\right)^{0,5}},$$

$$\frac{\mu_w}{\mathrm{Pr}_w}\frac{\partial H}{\partial n}\bigg|_w-\varepsilon_1\sigma T_w^4=-\lambda_1(1-\varphi)\frac{\partial T}{\partial n_1}\bigg|_w,\qquad 0\le s<s_1, \tag{1.7}$$

$$\frac{\mu_w}{\mathrm{Pr}_w}\frac{\partial H}{\partial n}\bigg|_w-\varepsilon_2\sigma T_w^4-(\rho v)_{2w}(h_w-h_c)=-\lambda_2\frac{\partial T}{\partial n_1}\bigg|_w,\quad s_1\le s\le s_{\text{к}},$$

$$J_{iw}+(\rho v)_{2w}c_{iw}=R_i,\qquad i=\overline{1,N-1},\qquad (\rho v)_{2w}=\sum_{i=1}^{N}R_i;$$

$$\left(\lambda_1(1-\varphi)\frac{\partial T}{\partial n_1}\right)\bigg|_{n_1=L_{\text{н}}}=(\rho v)_{1w}c_{pg}\frac{r_w}{(rH_1)_{n_1=L_{\text{н}}}}(T_{\text{н}}-T|_{n_1=L_{\text{н}}}),\quad 0\le s<s_1, \tag{1.8}$$

$$\lambda_2\frac{\partial T}{\partial n_1}\bigg|_{n_1=L}=0,\qquad s_1\le s\le s_{\text{к}},\qquad L=L_{\text{н}}-\int_0^t\omega\,dt;$$

$$\frac{\partial T}{\partial s}\bigg|_{s=0}=0,\quad \frac{\lambda_1(1-\varphi)}{H_1}\frac{\partial T}{\partial s}\bigg|_{s=s_1}=\lambda_2\frac{\partial T}{\partial s}\bigg|_{s=s_1},\quad \frac{\partial T}{\partial s}\bigg|_{s=s_{\text{к}}}=0; \tag{1.9}$$

$$T|_{t=0}=T_{\text{н}}. \tag{1.10}$$

In this statement of the problem the effective adiabatic exponent γ_e for air in chemical equilibrium is determined from [2], and air is used as the injected gas coolant. The products of ablation of the carbon conical section are assumed to dilute the air mixture weakly and to have insignificant influence on the transfer coefficients. If the Lewis numbers are assumed to be equal to unity, the heat flux $\frac{\mu_w}{\mathrm{Pr}_w}\frac{\partial H}{\partial n}\Big|_w$ is determined from the system of equations in the gaseous phase, and the diffusion fluxes J_{iw} are determined with recourse to the analogy between heat and mass transfer processes. The mass flow of gas from the surface of the porous nose section $(\rho v)_{1w}$ is assumed to be given or to be expressed in terms of the difference between the squares of the pressures in the empty interior of the shell and the outer edge of the boundary layer after integration of the Darcy equation. At the interface for $s \ge s_1$ we consider the kinetic diagram of nonequilibrium chemical reactions [3, 4]

$$\begin{array}{lll} C+O_2=CO_2, & 2)\ 2C+O_2-2CO, & 3)\ C+O-CO,\\ C+CO_2=2CO, & 5)\ O+O+C-O_2+C, & 6)\ N+N+C-N_2+C. \end{array}$$

The molar and mass velocities of the given chemical reactions are described in detail in [4], and the expression for the ejection mass velocity in ablation has the form

$$(\rho v)_{2w}=\rho_w\left[\left(\frac{m_6}{m_2}-1\right)c_{2w}B_1+\left(2\frac{m_5}{m_2}-1\right)c_{2w}B_2+\left(\frac{m_5}{m_1}-1\right)c_{1w}B_3+\left(2\frac{m_5}{m_6}-1\right)c_{6w}B_4\right]. \tag{1.11}$$

In Eq. (1.11) the components are enumerated in the order O, O_2, N, N_2, CO, CO_2, and

$$B_j=k_j\exp\left(-\frac{E_j}{RT_w}\right);\qquad \rho_w=\frac{p_e m_w}{RT_w}.$$

In these and subsequent equations $\bar{u}=u/u_e$ is the dimensionless velocity, $g=H/H_{e0}$ is the dimensionless enthalpy,

$$\xi = \frac{s}{R_N},\quad \eta = \frac{u_e r_w}{\left(2\int\limits_0^s \rho_e \mu_e u_e r_w^2\, ds\right)^{1/2}} \int\limits_0^n \rho\, dn$$

are the Dorodnitsyn–Lees variables,

$$\alpha = \frac{2\int\limits_0^\xi \rho_e \mu_e u_e r_w^2\, d\xi}{\rho_e \mu_e u_e r_w^2},\quad \beta = \frac{1}{u_e}\frac{du_e}{d\xi}\alpha$$

are dimensionless parameters, r and H_1 are the Lamé constants, n_1 is directed along the normal to the outer contour of the body into the depth of the material, φ is the porosity, ω is the linear velocity of the ablation surface,

$$h_w = \sum_{i=1}^{N} c_{iw} h_{iw},\quad m_w = \left(\sum_{i=1}^{N} \frac{c_{iw}}{m_i}\right)^{-1}$$

are the enthalpy of the mixture and the average molecular mass at the wall, L_{H} is the initial thickness of the shell in the flow, E_j and k_j are the activation energy and coefficient of the exponential function for the j-th heterogeneous reaction, c_i is the mass concentration of the i-th component, and R_N is the radius of the spherical nose section.

For the laminar, transition, and turbulent flow regimes in the boundary layer we have

$$l = \frac{\rho(\mu + \Gamma\mu_{\text{T}})}{\rho_e \mu_e},\qquad \text{Pr}_\Sigma = \frac{(\mu + \Gamma\mu_{\text{T}})\text{Pr}\text{Pr}_{\text{T}}}{\mu\text{Pr}_{\text{T}} + \Gamma\mu_{\text{T}}\text{Pr}}.$$

The subscripts e, $e0$, and w refer to the outer edge of the boundary layer, the stagnation point, and the surface of the body, the subscripts 1 and 2 identify the characteristics of the condensed phase of the spherical and conical sections of the body, the subscript g refers to the gaseous phase of the porous spherical shell, and T and H identify the turbulent transfer characteristics and the initial conditions. In the expression for the stream function f_w in (1.7), $(\rho v)_w$ assumes the values $(\rho v)_{1w}$ for $0 \le \xi < \xi_1$ and $(\rho v)_w = (\rho v)_{2w}$ for $\xi_1 \le \xi \le \xi_\kappa$.

To describe the turbulent flow, we use the two-layer, turbulent boundary-layer model described in detail and tested out in [6, 7]. In numerical integration Pr = 0.72, and $\text{Pr}_{\text{T}} = 1$. For the boundary-layer equation an iterative interpolation method [8] is used to generate combined differencing schemes that ensure matching of the unknown characteristics at the boundary of the laminar sublayer and the turbulent core and that take into account the behavior of μ_{T} across the boundary layer. This permits the calculations to be carried out over a wide range of Reynolds number and injected gas flow rates. The two-dimensional equations (1.4) and (1.5) are calculated by a decoupling method [9] in combination with the method of [8].

A computational algorithm has been constructed as follows with allowance for the quasisteady character of the processes in the gaseous phase: for given stagnation parameters and a known pressure distribution along the body, the values of the quantities at the outer edge of the boundary layer are determined, including the concentrations c_{ie}; for a given initial value $T_{w\text{H}}$ the system of equations (1.1)–(1.3) is calculated with allowance for the known distribution of $(\rho v)_{1w}$, and the heat flux to the surface of the body $\dfrac{\mu_w}{\text{Pr}_w}\dfrac{\partial H}{\partial n}\bigg|_w$ is determined; the conditions of conservation of mass of the components in (1.7) are used to find the composition of the gases at the wall c_{iw}, the enthalpy of the mixture at the wall h_w, and the ejection mass velocity $(\rho v)_{2w}$. Equations (1.4) and (1.5) are then calculated with the appropriate boundary and initial conditions, and the new surface temperature $T_w(\xi)$ is determined. The process is repeated by the above-described technique.

In solving the problem in the k-th phase, the time step is selected automatically on the basis of the specified accuracy; from 80 to 200 time steps are required to achieve a steady regime, depending on the incoming heat flux.

2. Calculations of flow past a spherically blunted 5° cone have been carried out for the testing conditions and model geometry in [10]: $M_\infty = 5$; $R_N = 0.0508$ m. Here the stagnation temperature T_{e0} is set equal to 4000 K, the stagnation pressure is varied from $3.125\cdot10^5$ N/m^2 to 10^6 N/m^2, and the flow rates of the gas coolant are varied from $(\rho v)_{1w}(s) = \text{const} = 1.626$ kg/(m^2·sec) to $(\rho v)_{1w}(s) = 13$ kg/(m^2·sec). The shell thickness L_{H} is assigned two values $2.2\cdot10^{-3}$ m and $15\cdot10^{-3}$ m. The thermophysical characteristics of the porous nose section correspond to steel: $\rho_1 c_1(1-\varphi) = 4.68\cdot10^6$ J/(m^3·K); $\lambda_1(1-\varphi) = 23$ W/(m·K). The thermophysical coefficients of the graphite material of the conical shell are specified from [11]. The emissivities are $\varepsilon_1 = 0.7$ and $\varepsilon_2 = 0.85$, the kinetic characteristics of the heterogeneous reactions are taken from [3, 12], and the enthalpy of graphite h_C is calculated according to an equation in [13].

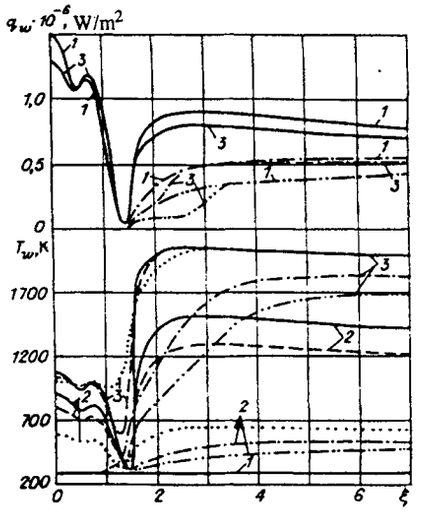

Fig. 1

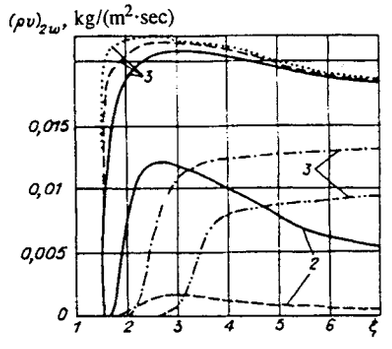

Fig. 2

Figures 1 and 2 show the distributions of the heat fluxes and the surface temperatures, along with the ejection mass velocities in the veil zone at different times. Here $p_{e0} = 3.125 \cdot 10^5$ N/m^2, curves 1 correspond to the initial time $t = 0$ ($T_w = T_H = 288$ K), curves 2 correspond to $t = 5$ sec, and curves 3 are plotted for the steady flow regime, which is attained at different times depending on the flow conditions and the length L_H. The dashed curves are plotted for $(\rho v)_{1w} = 1.626$ kg/(m^2·sec) and $L_H = 2.2 \cdot 10^{-3}$ m, the dotted curves for $(\rho v)_{1w} = 1.626$ kg/(m^2·sec) and $L_H = 15 \cdot 10^{-3}$ m, the dot-dash curves with single and double dots correspond to $L_H = 15 \cdot 10^{-3}$ m, $(\rho v)_{1w} = 6.5$ kg/(m^2·sec) and $(\rho v)_{1w} = 13$ kg/(m^2·sec), respectively, and the solid curves are plotted for the one-dimensional problem, which follows from Eqs. (1.4) and (1.5) without crossflow along the coordinate s for $(\rho v)_{1w} = 1.626$ kg/(m^2·sec) and $L_H = 2.2 \cdot 10^{-3}$ m.

It follows from Fig. 1 that, given the same flow rate $(\rho v)_{1w} = 1.626$ kg/(m^2·sec), the influence of heat flow and the initial shell thickness L_H is strongly felt at times close to the initial time [curves 2 for $T_w(\xi)$], and this fact can be exploited to lower the surface temperature at short times into the process. For the steady regime under the given conditions the influence of heat flow and L_H is felt in the region of the conical section just next to the porous nose section and also on the spherical part of the body. When the gas flow $(\rho v)_{1w}$ is increased (dot-dash curves with single and double dots), the heat fluxes in the veil zone behave monotonically, the temperature is lowered significantly at the junction of the spherical and conical sections, and a heat sink regime is established, draining from the conical part of the shell into the region of the porous nose section. Now the influence of heat flow is manifested on a large part of the veil zone, and the drop in the steady-state surface temperature from the radiation equilibrium temperature T_{wp} (solid curves 3 and 4 in Fig. 3) attains hundreds of degrees.

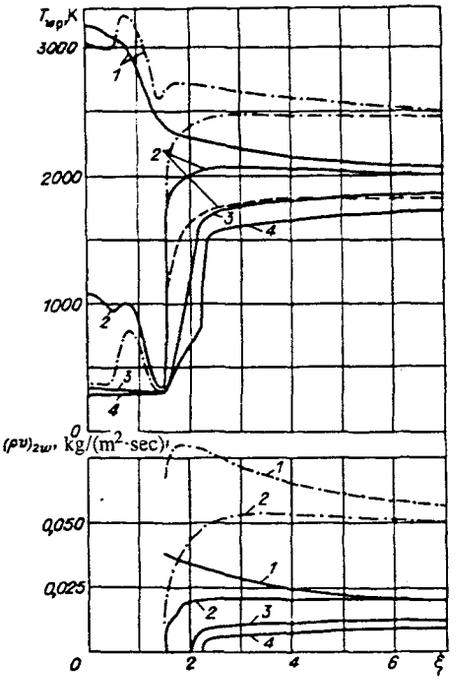

Fig. 3

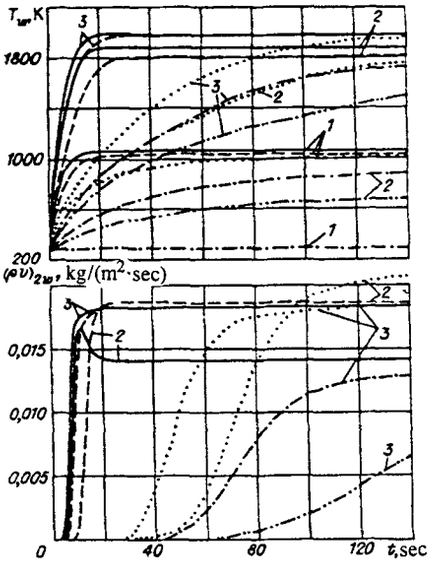

Fig. 4

As for the behavior of the heat flux around the circumference of the body at different times, its variation is complicated because of the nonmonotonic dependence of the enthalpy h_w on the temperature T_w. In this case, as T_w increases in the region of intense heterogeneous chemical reactions, the function $h_w(c_{iw}, T_w)$ has a minimum, whose position and value also depend on the heat transfer conditions, i.e., $\alpha/c_p = q_w/(H_{e0} - h_w)$. Consequently, the influence of the enthalpy factor h_w/H_{e0} on the heat flux depends on the position of the point ξ, the governing parameters of the problem, etc. In addition, the heat flux depends on $(\partial h_w/\partial\xi)/(H_{e0} - h_w)$ [14].

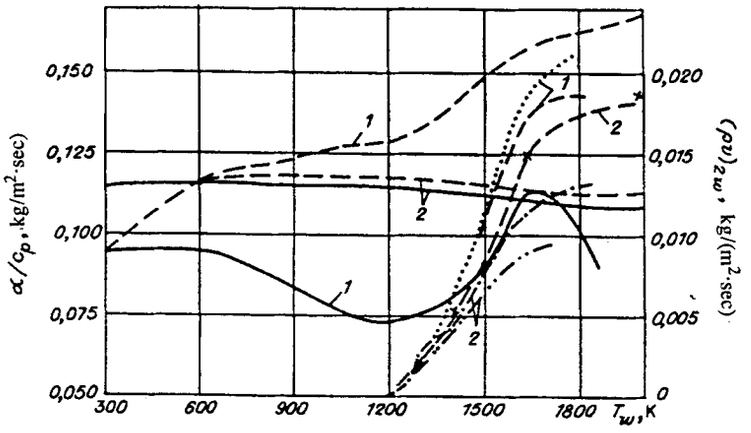

Fig. 5

It follows from Fig. 2 that the distributions of the ejection mass velocity $(\rho v)_{2w}$ associated with thermochemical ablation of the conical part of the body in the steady state qualitatively repeat the behavior of the convective heat fluxes toward the surface. Ablation is a minimum in the veil zone at the maximum temperature for $(\rho v)_{1w} = 1.626$ kg/(m^2·sec) (solid, dashed, and dotted curves in Fig. 2), and the maximum value of $(\rho v)_{2w}$ corresponds to the minimum temperature T_w for $L_H = 15 \cdot 10^{-3}$ m. This result is attributable to the fact that the process takes place in the diffusion regime at the given surface temperatures, where the value of $(\rho v)_{2w}$ does not depend on T_w but is associated with the value of the heat transfer coefficient α/c_p, which decreases as the surface temperature increases in the investigated range of T_w.

Thus, using reaction 2 in the kinetic scheme as the governing process [12] and assuming Fick's law for the diffusion flows, from Eqs. (1.7) and (1.11) we obtain

$$\begin{aligned} -\rho_w D \left.\frac{\partial c_2}{\partial n}\right|_w + (\rho v)_{2w} c_{2w} &= -k_2 c_{2w} \rho_w \exp\left(-\frac{E_2}{RT_w}\right), \\ -\rho_w D \left.\frac{\partial c_5}{\partial n}\right|_w + (\rho v)_{2w} c_{5w} &= 2k_2 c_{2w} \rho_w \frac{m_5}{m_2} \exp\left(-\frac{E_2}{RT_w}\right), \\ (\rho v)_{2w} &= k_2 c_{2w} \rho_w \exp\left(-\frac{E_2}{RT_w}\right)\left(2\frac{m_5}{m_2} - 1\right). \end{aligned} \tag{2.1}$$

Making use of the analogy between heat and mass transfer processes, we have

$$c_{2w} = \frac{c_{2e}(\alpha/c_p) - (\rho v)_{2w}\left(\frac{m_2}{2m_5 - m_2}\right)}{\alpha/c_p + (\rho v)_{2w}}.$$

For the determination of $(\rho v)_{2w}$ we then obtain

$$\left[\frac{(\rho v)_{2w}}{(\alpha/c_p)}\right]^2 + \frac{(\rho v)_{2w}}{(\alpha/c_p)}\left[1 + \frac{k_2 \rho_w \exp\left(-\frac{E_2}{RT_w}\right)}{(\alpha/c_p)}\right] = \left(2\frac{m_5}{m_2} - 1\right)\frac{c_{2e}k_2}{(\alpha/c_p)}\rho_w \exp\left(-\frac{E_2}{RT_w}\right). \tag{2.2}$$

For the diffusion regime $k_2 \exp(-E_2/RT_w) \to \infty$ we obtain the following from Eq. (2.2):

$$\frac{(\rho v)_{2w}}{(\alpha/c_p)} = \left(2\frac{m_5}{m_2} - 1\right)c_{2e}. \tag{2.3}$$

We note that a linear attenuation law for the heat transfer coefficient associated with the injection of ablation products can be used to reduce expressions (2.2) and (2.3) to the customary form for $(\rho v)_{2w}/(\alpha/c_p)^0$, where $(\alpha/c_p)^0$ is the heat transfer coefficient to an impermeable surface. A comparison of (2.2) and (2.3) with the results of solving the conditions of mass conservation of the components for the complete kinetic scheme indicates satisfactory accuracy of the analytical expressions obtained for the kinetic and diffusion regimes, where the concentration c_{2e} is taken equal to 0.23 as a consequence of the simplification of the kinetic scheme in (2.2) and (2.3).

As the mass flow of the gas coolant from the surface of the nose section increases, the convective heat flux in the veil zone and the surface temperature decrease, causing the ablation rate to drop significantly (dot-dash curves 3 with single and double dots, plotted for steady flow conditions). We also note that the abrupt variation of the ablation curve around the circumference of the cone (solid curve 2) is caused by the kinetic regime of the surface reactions at the given time.

To analyze the influence of heat flow, we augment the calculations of the problem in the conjugate formulation with numerical integration of the steady-state problem derived from the one-dimensional formulation of the equations in the condensed phase (1.4) and (1.5). In this case the energy conservation conditions from (1.7) have the form

$$\begin{aligned} &\frac{\mu_w}{\mathrm{Pr}_w}\frac{\partial H}{\partial n}\bigg|_w - \varepsilon_1\sigma T_{wp}^4 = (\rho v)_{1w}c_{pg}(T_{wp} - T_{\text{в}}), \qquad 0 \le s < s_1, \\ &\frac{\mu_w}{\mathrm{Pr}_w}\frac{\partial H}{\partial n}\bigg|_w - \varepsilon_2\sigma T_{wp}^4 - (\rho v)_{2w}(h_w - h_{\text{C}}) = 0, \qquad s_1 \le s \le s_{\text{к}}, \end{aligned} \tag{2.4}$$

where T_{wp} for $s \ge s_1$ corresponds to the equilibrium radiation temperature.

Figure 3 gives the distributions of T_{wp} and the ejection mass velocities on the conical section $(\rho v)_{2w}$ for various values of $(\rho v)_{1w}$ and various stagnation pressures. Here the solid curves 1–4 correspond to $p_{e0} = 3.125\cdot10^5$ N/m^2 and $(\rho v)_{1w} = 0$, 1.626, 6.5, 13 kg/(m^2·sec), the dashed curve 2 is plotted for $(\rho v)_{1w} = 1.626$ without heterogeneous chemical reactions, and the dot-dash curves 1 and 2 correspond to $p_{e0} = 10^6$ N/m^2, $(\rho v)_{1w} = 1.626$ kg/(m^2·sec) and $(\rho v)_{1w} = 4.88$ kg/(m^2·sec), respectively. As should be expected, agreement is observed between the results represented by the solid curves 2 in Fig. 3 and the data of Figs. 1 and 2 (solid curves 3), which are obtained in the limit $t \to \infty$ for the one-dimensional case in the condensed phase.

An increase in the stagnation pressure causes the turbulent viscosity μ_T to increase and, as a result, the convective heat fluxes to the body, the temperature T_{wp}, and the ablation rates $(\rho v)_{2w}$ increase as well. The behavior of q_w and T_{wp} changes qualitatively in the region of the porous nose section, where the maximum values of the heat fluxes and the temperatures T_{wp} correspond to $\xi \approx 0.75$.

It follows from these calculations and from Fig. 3 that the behavior of the convective fluxes q_w, the temperatures T_{wp}, and the ablation rates $(\rho v)_{2w}$ along the generatrix of the body are qualitatively identical. Notice also the contribution of heterogeneous chemical reactions, which cause the radiative surface temperature T_{wp} to rise significantly under the given conditions; this follows from a comparison of the solid and dashed curves 2.

On the whole, the indicated model can be used for on-line computations of the maximum temperature levels T_{wp} in the zone of the gas veil and the ablation rate $(\rho v)_{2w}$; however, a comparison with the data of Figs. 1 and 2 shows that the influence of heat flow can become decisive for any number of conditions, particularly in the transition zone between the spherical and conical sections.

In accordance with the designation of the curves in Figs. 1 and 2, Figure 4 shows the dynamics of the time variation of the surface temperature and the ejection mass velocity in different cross sections along the generatrix (curves 1–3 for ξ = 0, 1.7, 7). Clearly, as the thickness of the shell increases and the heat flux decreases, the increase in the flow rate $(\rho v)_{1w}$ has the effect of greatly prolonging the time for the process to reach the steady flow regime. For example, on the conical section this time is 420 sec for $(\rho v)_{1w} = 13$ kg/(m^2·sec) and $L_{\text{H}} = 15\cdot10^{-3}$ m (dot-dash curves with double dots). In regard to the ejection mass velocity, it is interesting to note the nonmonotonic behavior of $(\rho v)_{2w}$ with time in the cross section $\xi = 1.7$ (solid curve 2). At $t = 10$ sec the surface temperature exceeds 1650 K in this case, and the regime of heterogeneous reactions approaches the diffusion regime. The reduction in $(\rho v)_{2w}$ at later times is caused by a decrease in the heat transfer coefficient α/c_p, for which the time behavior of the temperature T_w is also typically nonmonotonic. We note that the burnup depth $\int_0^t \omega\, dt$ for the results in Figs. 2 and 4 at $\xi = 7.0$ for the dashed curves is equal to $1.45\cdot10^{-3}$ m at the time $t = 200$ sec.

It follows from these results that different thermochemical ablation regimes can occur at equal times in the veil zone on the conical section of the body. For example, a diffusion regime is attained in steady flow for regions of the conical section far from the spherical nose, whereas a kinetic regime occurs in the zone next to the nose section. This follows from the processing of several results of solving the problem in the conjugate setting in the form of $(\rho v)_w$ as a function of T_w, plotted in Fig. 5, where curves 1 and 2 are obtained for $\xi = 1.7$ and $\xi = 7$. We observe agreement between the computed data and

the results of solving Eqs. (2.2) and (2.3) analytically (represented by ×'s); this fact can be utilized to estimate the ejection mass velocity. It should be recalled that the main difficulty here is to determine the heat transfer coefficient in the veil zone.

As an illustration, Fig. 5 shows the results of processing the particular set of data represented by the solid curves in Fig. 1 to obtain α/c_p as a function of T_w in the above-indicated cross sections ξ (solid curves 1 and 2). Also shown in this figure, with a view toward analyzing the influence of the nonisothermal surface on q_w and α/c_p, are the results of processing the calculations with parametric sequential inspection of all $T_w(\xi)$ = const for the case of a thermochemically reactive conical surface (dashed curves 1 and 2).

A comparison shows that the heat transfer coefficients are close in the peripheral region of the conical section $\xi = 7$, and the functions $\frac{\alpha}{c_p}(T_w)$ plotted for isothermal conditions can be used in this region. For cross sections close to ξ_1 we find that α/c_p is a complex function, whose form is associated, on the one hand, with the nonmonotonic behavior of h_w and, on the other, with the strong dependence on the quantity $\frac{\partial h_w}{\partial \xi}/(H_{e0} - h_w)$, because it has been shown [6, 14] that the structure of the heat transfer coefficient in general has the form $\alpha/c_p = f_1(h_w/H_{e0}) - f_2(h_w/H_{e0})\frac{\partial h_w}{\partial \xi}/(H_{e0} - h_w)$. The growth of α/c_p with T_w for isothermal conditions at the wall, in turn, is attributable to the monotonic decrease of h_w with increasing ξ on the conical section in the region adjacent to ξ_1, where $\frac{\partial h_w}{\partial \xi}/(H_{e0} - h_w)$ increases in absolute value with increasing temperature T_w. Under the investigated conditions the second term exerts the predominant influence, causing α/c_p to vary as indicated.

In summary, it is recommended that the conjugate formulation of the problem be used to find the characteristics of heat and mass transfer and thermochemical ablation in the region of abrupt variation of the functions around the circumference of a body as a consequence of the thermal veil.

REFERENCES

1. V. I. Zinchenko, A. G. Kataev, and A. S. Yakimov, "Thermal regimes of bodies in flows with gas injection from the surface," Prikl. Mekh. Tekh. Fiz., No. 6 (1992).
2. I. N. Murzinov, "Laminar boundary layer on a sphere in hypersonic flow of equilibrium-dissociating air," Izv. Akad. Nauk Mekh. Zhidk. Gaza, No. 2 (1966).
3. A. M. Grishin and V. M. Fomin, Conjugate and Transient Problems in the Mechanics of Reacting Media [in Russian], Nauka, Novosibirsk (1984).
4. V. I. Zinchenko and A. S. Yakimov, "Thermochemical ablation regimes of a carbophenol composite under the influence of heat flux," Fiz. Goreniya Vzryva, **24**, No. 2 (1988).
5. T. Cebeci, "Behavior of turbulent flow near a porous wall with pressure gradient," AIAA J., **8**, No. 12 (1970).
6. V. I. Zinchenko, Mathematical Modeling of Conjugate Heat and Mass Transfer Problems [in Russian], Izd. Tomsk. Univ., Tomsk (1985).
7. A. V. Bureev and V. I. Zinchenko, "Calculation of flow past a spherically blunted cone for various flow regimes in the shock layer and gas injection from the surface," Prikl. Mekh. Tekh. Fiz., No. 2 (1991).
8. A. M. Grishin, V. N. Bertsun, and V. V. Zinchenko, The Iterative Interpolation Method and Its Applications [in Russian], Izd. Tomsk. Univ., Tomsk (1961).
9. N. N. Yanenko, Method of Fractional Steps for the Solution of Multidimensional Problems of Mathematical Physics [in Russian], Nauka, Novosibirsk (1987).
10. R. N. Feldhuhm, "Heat transfer from a turbulent boundary layer on a porous hemisphere," AIAA Paper No. 119, AIAA, New York (1976).
11. V. P. Sosedov, Properties of Carbon-Based Construction Materials: Handbook [in Russian], Metallurgiya, Moscow (1975).
12. L. V. Khanter, L. L. Perini, O. V. Conn, and P. T. Brenza, "The method of ablation computation of graphite coating of re-entrying aircraft at subsonic and supersonic velocities," Aerocosmic Tech., No. 8, 31-37 (1987).

13. L. M. Buchnev, A. I. Smyslov, I. A. Dmitriev, et al., "Experimental study of the enthalpy of a graphite quasi-single crystal and carbon fiber-reinforced glass in the temperature interval 300-3800 K," Teplofiz. Vys. Temp., **25**, No. 6 (1987).
14. V. I. Zinchenko, "Characteristics of conjugate heat and mass transfer in supersonic and hypersonic flows around blunt bodies," Izv. Vyssh. Uchebn. Zaved. Fiz., **35**, No. 8 (1992).